

Random Telegraph Noise Pixel Classification and Time Constant Extraction for a 1.1 μm Pitch 8.3MP CMOS Image Sensor

Calvin Chao, Honyih Tu, Thomas Wu, Kuo-Yu Chou, Shang-Fu Yeh, and Fu-Lung Hsueh
 Taiwan Semiconductor Manufacturing Company, Hsinchu, Taiwan, ROC
 Tel: (886) 3-5636688 ext 703-8243, email: calvin_chao@tsmc.com

Introduction

In a well-designed CIS with the pinned photodiode pixels, the reset noises can be cancelled by the correlated double sampling (CDS) and the downstream circuit noises can be effectively suppressed by using low-noise, high-gain column amplifiers. The remaining readout noises typically show a long tail distribution dominated by the random telegraph noises (RTN) [1]-[6] from the pixel source followers (SF) and the column circuits. In the dark region of a video, the RTN pixels appear to be twinkling and blinking, causing unpleasant visual artifacts; thus degrading the video image quality. Therefore, it is important to understand, to characterize, and to minimize the RTN in CIS.

In this paper, we study the RTN of a 1.1 μm pixel, 8.3MP CIS fabricated in a 45nm BSI process. The simplified signal chain and the timing control are shown in Fig. 1. The 2-by-2 shared pixel has a FWC around 6000e⁻ and an average conversion gain of 120 $\mu\text{V}/\text{e}^-$; corresponding to a 1.34fF floating diffusion (FD) capacitance. The column amplifier gain is programmable from 1X to 8X. The circuit noise can be measured independently without the pixels in a special test mode. The SF is a low-V_t device with a size of W = 0.2 μm , L = 0.8 μm .

RTN Pixel Classification

The random noises (RN) measured in the dark have a non-Gaussian distribution with a notable long tail as exemplified in Fig. 2. Although the median RN is only 1.5e-rms under the 8X gain, the RN in the histogram tail could be as high as 27e-rms. The column circuit with RTN affects all the pixels on the same column and can be identified easily. Such columns are removed in the statistical plots in order to focus on the pixel RTN only. A majority of the noisy pixels in the long tail region show the signature behavior of a single-trap RTN with 3 clearly identifiable peaks in the histograms because of the CDS operation. Several examples of the 3-peak pixels are given in Fig. 3. A variety of other types of pixels are also observed as in Fig.4. We have verified that the RTN of the pixels sharing the same SF are strongly correlated, indicating that the SF is indeed the major source of RTN.

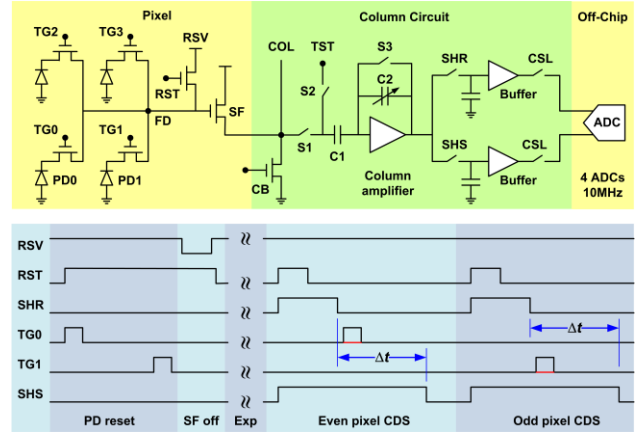


Figure 1. Top: the simplified signal chain of the CIS test chip. Bottom: the pixel operation timing diagram. In the dark test mode, the TG0 and TG1 during pixel readout are tuned off; the Δt can be programmed from 0 to 25 μs in 0.1 μs steps.

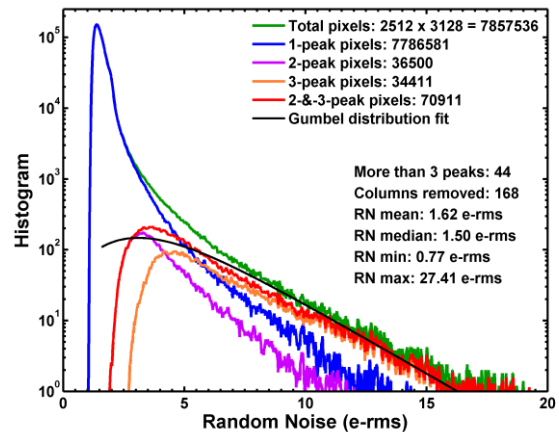


Figure 2. The noise distribution of the 8.3MP array in the dark with 168 RTN columns removed. The pixels are sorted into 4 groups according to the number of peaks identified in the 5,000 frame histograms.

Most of the previous RTN studies in the literature involved limited sample sizes or non-CIS processes. Here for the first time we analyzed every pixel in an entire 8.3MP array and classified them into 4 categories according to the number of observable peaks found in the 5,000-frame signal histograms. For a single-trap RTN, if the trap occupancy probabilities are the same in the reset sampling (SHR) and the signal sampling (SHS) phases of the CDS, the resulting histograms would show 2 equal side peaks

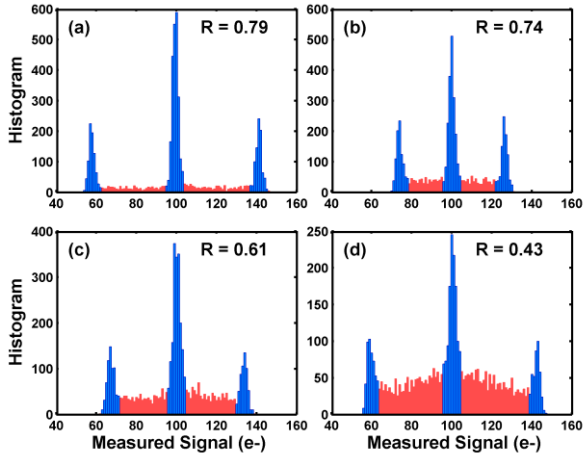


Figure 3. Pixels showing the signature behavior of a single-trap RTN with 3 distinctive peaks in the signal histograms. The “settling ratio” R is defined as the ratio of the blue area versus the total area (blue + red).

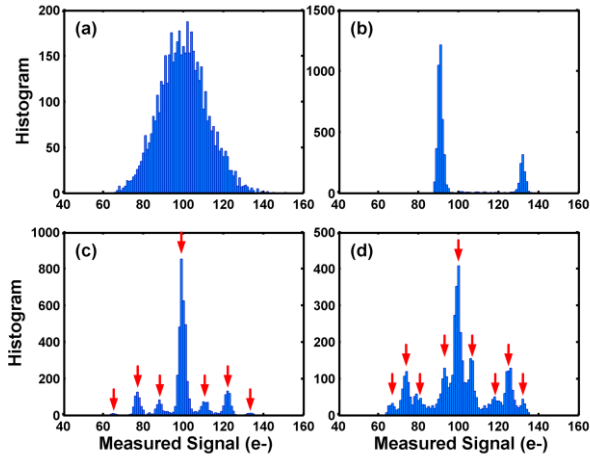


Figure 4. A variety of noisy pixels showing (a) 1 peak only, (b) 2 peaks, (c) 5 or 7 peaks, and (d) 9 peaks in the signal histograms.

symmetrically on the higher and lower sides of the center main peak. But for the pixel without the row-select device, the SF needs to be turned OFF (the channel is biased in the accumulation regime) during the charge integration by pulling low the FD voltage (setting RST to high and RSV to low), and turned ON (the channel is biased in the inversion regime) during the CDS, as described in the Fig. 1 timing diagram. Some of the electrons traps are emptied when the channel is populated with holes under the accumulation condition, and have less time to reach the steady state in the first sampling (SHR) than in the second sampling (SHS) [2], [7]. Due to this asymmetry, some single-trap pixels showed 3 asymmetrical peaks, and some showed only 2 peaks. The physical reasons why some pixels behave differently from the others are still under investigation.

In Figs. 2, 5, and 7, the single-trap RTN pixels (the 2- and 3-peak pixels) account for about 1% of the total population. The pixels having multiple traps are very rare; only 44 are found in this sample. However,

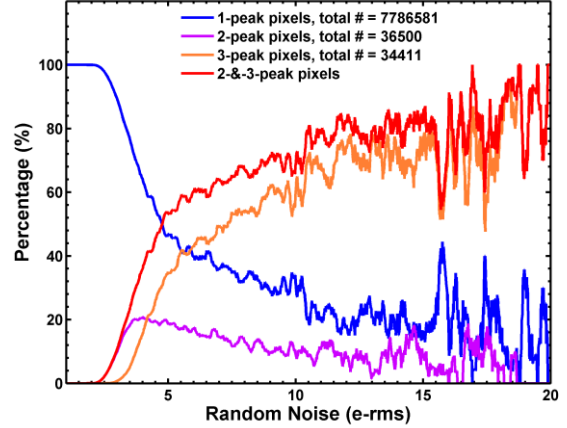


Figure 5. The percentage of pixels showing 1 peak, 2 peaks, and 3 peaks depends on the random noise magnitude. In the high noise region (>10 e-rms), clearly the 2- and 3-peak pixels dominate (single-trap RTN).

in the high noise region (>10 e-rms), the single-trap RTN percentage is as high as 70% to 90%. Similar percentages are found in many other chips. Evidently the long tail of the RN distribution is dominated by the single-trap RTN pixels, which can be described by a Gumbel [8] probability density function (PDF):

$$p(x) = \frac{1}{\beta} \exp(-z - e^{-z}); z = (x - \mu)/\beta, \quad (1)$$

where μ is the mean; the standard deviation is $\beta\pi/\sqrt{6}$.

On-Chip RTN Time Constant Extraction

We developed a new method for on-chip RTN time constant extraction using the double sampling circuits [6]. In this design, the time difference Δt between the double sampling can be programmed from 0 to $25\mu\text{s}$ in $0.1\mu\text{s}$ steps while turning off the TG in dark RN measurements. When the Δt is set to $0\mu\text{s}$, the two samplings (SHR and SHS) are essentially correlated with respect to the SF noises; therefore, the SF RTN are completely cancelled and the median RN is as low as 0.21e-rms . When the Δt is gradually increased towards $25\mu\text{s}$, the two samplings become increasingly uncorrelated. The resulting RTN transition from the correlated to the uncorrelated double sampling can be described by a time-dependent equation [6]:

$$n_{RTN}(t) = \frac{\sqrt{2\tau_e\tau_c}}{\tau_e + \tau_c} (\Delta V) \sqrt{1 - e^{-t/\tau_s}}; \tau_s = \frac{\tau_e\tau_c}{\tau_e + \tau_c}, \quad (2)$$

where τ_e and τ_c are the emission and capture time constant of a binary-state RTN trap; τ_s is defined as the characteristic time constant. The formula (2) can be derived from a differential equation based on a continuous-time model or from the probability functions based on a discrete-event model [6].

The family of curves in Fig. 6 and Fig. 7 show the evolution of the noise histograms and the inverse cumulative distribution functions (ICDF) from $\Delta t = 0$

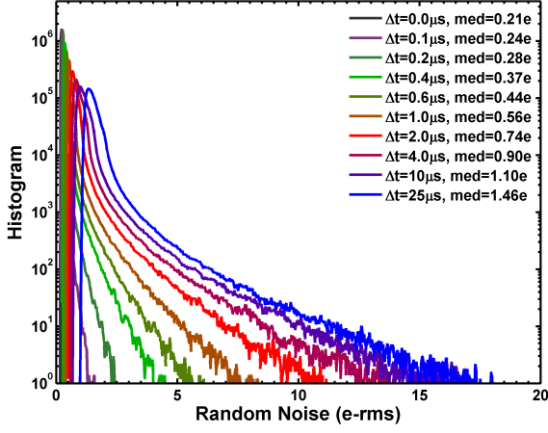


Figure 6. The random noise histograms with the double sampling time difference Δt gradually increased from 0 to 25 μs . At $\Delta t = 0 \mu\text{s}$, the readout circuit showed a very low noise of 0.21e-rms when the SF noises are cancelled by CDS.

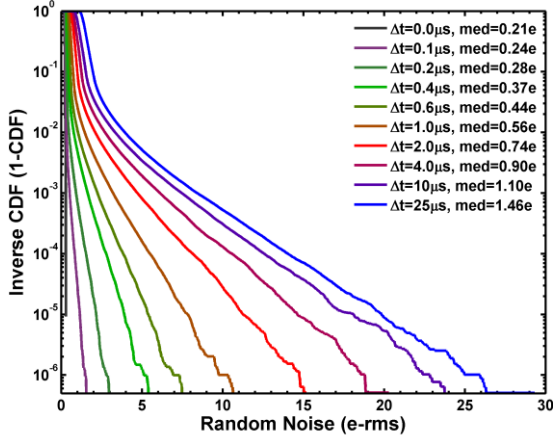


Figure 7. The inverse cumulative distribution functions (ICDF) of the random noises with the double sampling Δt gradually increased from 0 to 25 μs .

to 25 μs , respectively. In the case of $\Delta t = 0$, the SF noises are cancelled by CDS. The remaining median noise is 0.21e-rms. When Δt increases to 25 μs , the median noise increases to 1.48e-rms. It proves that the overall readout noises of this chip are primarily from the SF. The curve of $\Delta t = 25 \mu\text{s}$ in Fig. 7 shows that approximately 1% of the total population have noises higher than 4.2e-rms and 0.1% higher than 8.6e-rms.

The family of constant ICDF contours in Fig. 8 can be fit by Eq. (2) reasonably well with a common characteristic time constant. Furthermore, the time constant τ_s of each individual pixel can be practically extracted by fitting Eq. (2) to the measured RN as a function of Δt . Fig. 9 illustrates the fitting of several groups of pixels with τ_s in different ranges.

Fig. 10 shows the τ_s distribution of the noisiest 1,000 pixels measured at 1X and 8X gains, respectively. The majority of the time constants fall within the range from 1 μs to 500 μs . We noted that the time

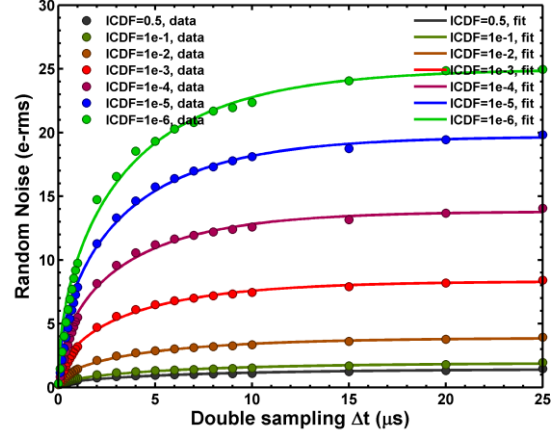


Figure 8. The constant ICDF contours at 0.5 (median), 1e-1, 1e-2, 1e-3, 1e-4, 1e-5, and 1e-6 as functions of Δt are well fit by the theoretical formula (2).

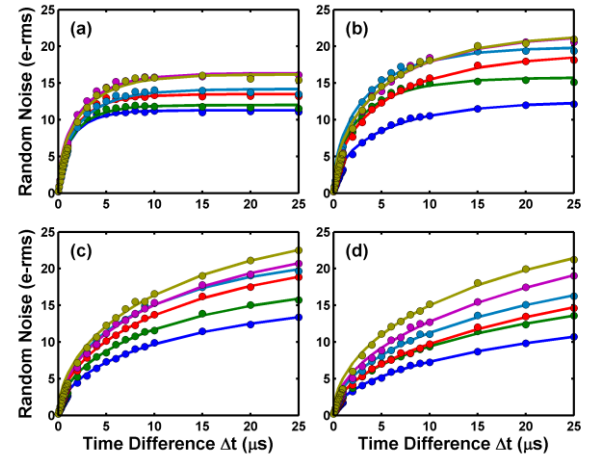


Figure 9. Selected subsets of pixels showing a variety of time constants extracted by curve fitting; (a) $\tau_s < 4 \mu\text{s}$, (b) $4 \mu\text{s} < \tau_s < 10 \mu\text{s}$, (c) $10 \mu\text{s} < \tau_s < 30 \mu\text{s}$, (d) $30 \mu\text{s} < \tau_s$.

constants longer than 100 μs might not be accurately extracted due to the limited range of curve fitting (25 μs). On the other hand, the time constants shorter than 5 μs are affected by the finite circuit bandwidth and settling time.

RTN Histogram Settling Ratio

Among the noisiest 1,000 pixels, about 80% show 3 peaks and about 15% show 1 peak. Interestingly, Fig. 10 shows that the 1-peak pixels tend to have shorter time constants, suggesting that some of the 1-peak pixels actually have 3 peaks (i.e., single-trap) but cannot be resolved due to the circuit bandwidth limitation.

Eq. (2) is based on an ideal assumption that the single RTN trap is either in an occupied state or an empty state, not in between. However, in the real circuits, the transition time between the occupied and empty states may be very short, but the circuits always have finite response time determined by the bandwidth. Inevitably, any unsettled signal values

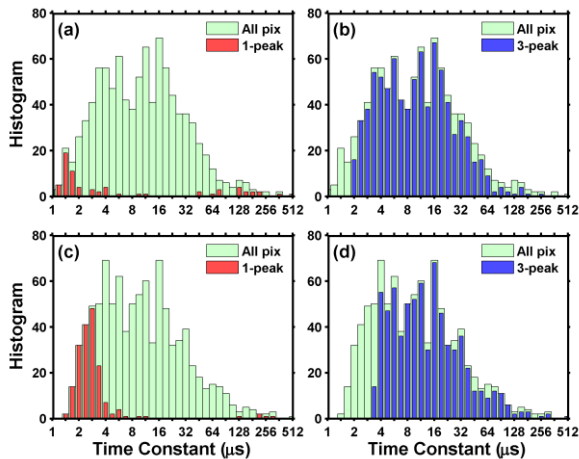


Figure 10. The distributions of the extracted time constants at 1X gain in (a) and (b); 8X gain in (c) and (d), for 1-peak and 3-peak pixels, respectively.

between the two well defined discrete states may also be captured during the measurement. The unsettled data points are highlighted as the red area in Fig. 3.

Accordingly, in Fig. 3, we define a “settling ratio” for the 3-peak histogram as the ratio of the number of the settled points (the blue area) vs. the total sample size (the sum of the blue and the red area). Intuitively, we expect that the settling ratio depends on the time constants of both the circuits and the RTN traps.

The settling ratios are plotted against the RTN time constants for the 1,000 noisiest pixels in Fig. 11, under the 1X and 8X gains. The settling ratios approach 100% for pixels with longer time constants, but decrease sharply for pixels with shorter time constants. For the same pixel with a fixed time constant, the settling ratio is higher at 1X gain than that at 8X gain. Because the column amplifier bandwidth, determined by the ratio of the feedback capacitance C_2 and the sampling capacitance C_1 , is higher at 1X gain than that at 8X gain.

To understand the data, we developed a RTN behavior model in MATLAB to simulate the settling ratio dependence on the time constant. First, we generate an ideal random telegraphic waveform for a single-trap RTN using random numbers for a given pair of emission and capture time constants with a large number of emission-capture transitions. Second, the time-domain waveform is transformed into the frequency domain using the FFT, multiplied by a low-pass filter corresponding to the circuit time constant, and transformed back to the time domain using the inverse FFT. Then, the periodically sampled RTN histogram and the settling ratio can be calculated from the resulting telegraphic waveform. Fig. 12 shows that the data in Fig. 11 can be reasonably reproduced by the RTN behavior model, where the circuit time constants at 1X and 8X gains are

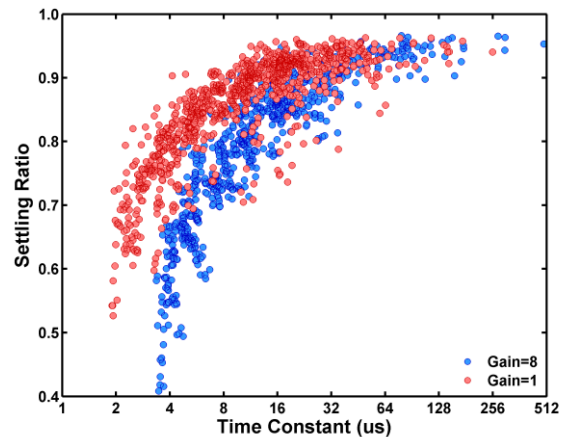


Figure 11. The RTN settling ratios of all 3-peak pixels vs. the time constants measured at 1X and 8X gain, respectively.

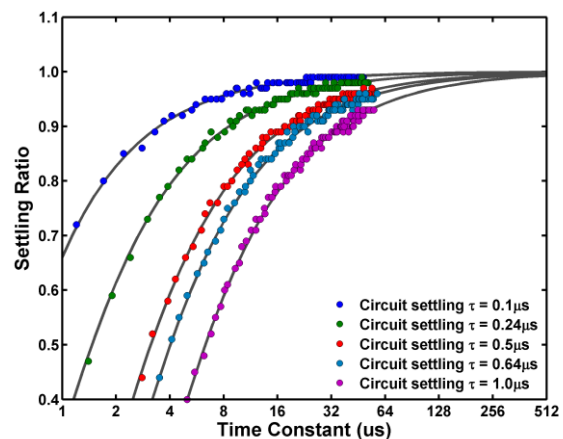


Figure 12. The MATLAB simulated RTN settling ratio vs. the characteristic time constant τ_s under various circuit settling time constants.

approximately $0.24\mu\text{s}$ and $0.64\mu\text{s}$, respectively, from circuit simulation.

Conclusions

In summary, a new on-chip RTN time constant extraction method was developed, based on the relaxation from the correlated to the uncorrelated double sampling. The pixels of an 8.3MP array are sorted into four different groups according to the number of observable RTN traps. The effects of circuit bandwidth on RTN settling ratio and time constant extraction were studied and accounted for in MATLAB behavior simulation.

Reference

- [1] J. Janesick et al., Proc. SPIE, vol. 7742, 2006.
- [2] X. Wang et al., IEDM, 2006, pp. 115-118.
- [3] K. Abe et al., IISW, 2007, pp. 62-65.
- [4] T. Obara et al., JJAP, Vol.53, 2014, pp. 04EC19.1-7.
- [5] R. Kuroda, ICMTS, 2016, pp. 46-51 (and references therein)
- [6] C. Chao et al., J-EDS, vol. 5, no. 1, 2017, pp. 79-89.
- [7] M.F. Snoeij et al., Workshop on CCD & AIS, 2005.
- [8] C. Walck, “Handbook on statistical distributions for experimentalists,” Stockholm, Sweden, 2007, Ch. 15, pp. 57-60.